Journal of Korean Powder Metallurgy Institute
Vol. 8, No. 3, 2001

Platinum Nano-Dispersion via *In Situ* Processing - Preparation and Catalytic Property of Porous $CaZrO_3$/MgO/Pt Nanocomposite -

Yoshikazu Suzuki, Hae Jin Hwang, Naoki Kondo and Tatsuki Ohji
Synergy Materials Research Center, National Institute of Advanced Industrial Science and Technology (AIST), Nagoya 463-8687, Japan
(Received August 3, 2001)

Abstract A bulk porous $CaZrO_3$/MgO composite with platinum nano-dispersion was synthesized in air atmosphere through the combination of several *in situ* reactions, including the pyrolysis of PtO_2. A mixture of $CaMg(CO_3)_2$ (dolomite), ZrO_2, PtO_2 and LiF (0.5 wt%, as an additive) was cold isostatically pressed at 200 MPa and sintered at 1100°C for 2 h. The porous $CaZrO_3$/MgO/Pt composite ($CaZrO_3$/MgO : Pt = 99 : 1 in volume) had a uniformly open-porous structure (porosity: 56%) with three-dimensional (3-D) network and a narrow pore-size distribution, similarly to the porous $CaZrO_3$/MgO composites reported before. Catalytic properties (viz., NO direct decomposition and NO reduction by C_2H_4) of the $CaZrO_3$/MgO/Pt composite were investigated up to 900°C. In the absence of oxygen, the NO conversion rate reached ~52% for the direct decomposition and ~100% for the reduction by C_2H_4, respectively. The results suggest the possibility of the porous composite as a multifunctional filter, i.e., simultaneous hot gas-filtering and de-NO_x in one component.

Keywords : Platinum, Nano-dispersion, In situ processing, Catalytic properties, NO_x

1. Introduction

Hot-gas cleaning is indispensable to various combustion and power applications.[1-4] Porous ceramics play key roles both for the physical filtration of soot[3-5] and for the chemical decomposition of toxic species (e.g., de-NO_x or de-SO_x) as catalysts themselves[6,7] or supports.[8]

The present authors have recently developed uniformly porous $CaZrO_3$/MgO composites with a 3-D network structure via reactive sintering method.[9,10] The pore-size distribution was very narrow (with pore size ~1 μm), and the porosity was controllable (typically ~30-50%) by changing the sintering temperature.[9] Due to their unique open-porous structure, they can be applied not only for filter materials but also for catalytic supports.

More recently, we have succeeded in dispersing platinum nano-particles into the above-mentioned porous materials by using a simple *in situ* processing technique, that is, the pyrolysis of platinum dioxide.[11] Since PtO_2 thermally decomposes into metallic platinum under the ordinary air atmosphere, this *in situ* process does not require a reductive-gas furnace. Other advantages of this process are that (1) starting PtO_2 particles can be more easily refined by ball-mill processes than metallic Pt particles (if it is used as a starting material itself), and (2) there is no toxic gas emission during the heating process, compared with the use of platinum salts or platinum complexes as Pt-source.

In this paper, we demonstrate the platinum nano-dispersion via *in situ* processing in more detail. Although we used a specific system as a base material (i.e., $CaZrO_3$/MgO porous composite), this Pt-nano-dispersion method can be applicable for variety of ceramic systems.

2. Experimental

2.1. Pyrolysis behavior of PtO_2

The pyrolysis of a commercial PtO_2 powder (Kojundo Chemical Laboratory Co., Ltd., 99.9%) was studied via thermogravimetry and differential thermal analysis (TG-DTA, 10°C/min) up to 1200°C in static air atmosphere. X-ray diffractometry (Cu-K_α at 40 kV and 100 mA) was used for characterizing the PtO_2 powder as well as the composite produced.

2.2. Preparation of bulk porous composite with Pt nano-dispersion

Natural $CaMg(CO_3)_2$ (high purity, $<75\ \mu m$[12,13]), ZrO_2 (un-doped, Sumitomo Cement Co. Ltd., 99.9%), LiF (Wako Pure Chemical Ind. Ltd., 99.9%) and above-mentioned PtO_2 powders were used as starting materials; 50 : 50 mol% of $CaMg(CO_3)_2$ and ZrO_2 with PtO_2 adjusted to give a composition of $CaZrO_3$/MgO : Pt = 99 : 1 vol% after sintering. LiF (0.5 wt% to total starting powders) was added to form a liquid phase during sintering to enhance reactivity and neck-growth.[9] The powders were wet-ball milled in ethanol for 6 h in a planetary ball-mill (acceleration: 6 G). The mixed slurry was dried, subsequently dry-ball-milled for 24 h, and sieved through a 100-mesh screen. The mixed powder was cold isostatically pressed at 200 MPa after mold-pressing. The green compacts (15 mm in diameter and ~5 mm in thickness) were sintered in air at 1100°C for 2 h to obtain the porous composite.

2.3. Characterization of bulk porous composite with Pt nano-dispersion

The microstructure was characterized by scanning electron microscopy. The porosity and the pore-size distribution were determined by mercury porosimetry (Poresizer 9320, Micromeritics, Norcross, GA). Mercury intrusion was carried out at pressures between 0 to 207 MPa.

NO decomposition was examined up to 900°C at atmospheric pressure in a quartz microreactor. Gas mixtures of 1000 ppm NO balanced by He (with or without 500 ppm C_2H_4 as a reducing agent) were passed through the microreactor containing 3 g of the porous $CaZrO_3$/MgO/Pt composite (containing 141 mg of Pt) at a flow rate of 50 ml/min. NO decomposition was detected using a chemiluminescent NO-NO_x analyzer (BSU-100 uH, Best Instrument) and also confirmed by a gas chromatograph (CP-2002, Chrom-pack).

3. Results and Discussion

3.1. Pylolysis behavior of PtO_2

Figures 1(a) and (b) show XRD pattern and TG-DTA diagrams of the PtO_2 powder. As can be seen from Fig. 1(a), the powder consisted of hexagonal α–PtO_2 with some amorphous PtO_2. The color of the as-received PtO_2 powder was dark brownish-gray, which suggests the co-existence of dihydrate ($PtO_2 \cdot 2H_2O$, brown) and monohydrate ($PtO_2 \cdot H_2O$, black) as well as anhydride (black).[14]

In Fig. 1(b), during the heating of the PtO_2 powder, weight losses of steep (~100°C), shallow (~100°C - ~620°C), very steep (~620°C - ~680°C), and then shallow (~680°C ~ 1100°C) slopes were observed. Thus, the first weight loss (and the corresponding endothermic peak) would be due to the desorption of the adsorbed water and the dehydration of crystalline water of dihydrate (i.e., $PtO_2 \cdot 2H_2O \rightarrow PtO_2 \cdot H_2O + H_2O$). The second weight loss (at ~100°C - 620°C) is attributable to the dehydration of crystalline water of monohydrate as well as the partial decomposition of the dioxide. Note that platinum has several lower oxidation states.[15,16] The third significant weight loss and the large endothermic peak are attributed to the pyrolysis of platinum dioxide. The deoxidation continued at the temperatures higher than ~680°C, and it was completed at ~1100°C. The weight loss from 100 to 1150°C was 16.4%, which agreed well with that in the ideal reduction, $PtO_2 \rightarrow Pt + O_2$. Without distinction of the adsorbed and crystalline water, the PtO_2 powder used can be nominally expressed as $PtO_2 \cdot 0.26H_2O$ from the TG-DTA analysis.

The TG-DTA result of the pyrolysis reaction, $PtO_2 \cdot Pt + O_2$, is consistent with the reported thermodynamic

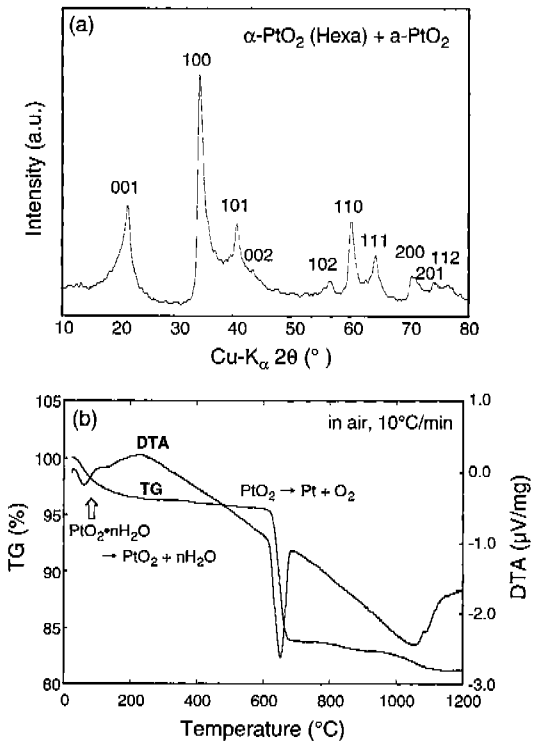

Fig. 1. Characterization of a PtO_2 powder: (a) XRD pattern and (b) TG-DTA diagrams indicating pyrolysis behavior in air atmosphere.

Table 1. Estimated Gibbs free energy change (ΔG) and equilibrium constant (K), supposing the O_2 as perfect gas under 1 atm pressure.

$PtO_2 = Pt + O_2(g)$			
T (°C)	ΔG (kJ)	K	Log (K)
200	49.981	3.032E-6	-5.518
300	32.513	1.088E-3	-2.963
400	15.213	6.598E-2	-1.181
500	-0.423	1.068E+0	0.029
600	-14.524	7.395E+0	0.869
700	-28.340	3.321E+1	1.521
800	-41.908	1.097E+2	2.040
900	-55.262	2.889E+2	2.461

data; the Gibbs free energy change and the equilibrium constant of the reaction are summarized in Table 1, calculated by using HSC Chemistry database.[17]

3.2. Phases and microstructure of the Pt-dispersed porous composite

Figure 2 indicates an XRD pattern of the porous $CaZrO_3$/MgO/1 vol%-Pt composite sintered at 1100°C. The XRD analysis revealed that it consisted of $CaZrO_3$, MgO and metallic platinum.

Note that the porosity of the *in situ* composites can be controlled by changing not only the sintering temperature but also the CO_2 partial pressure during the sintering.[10] The use of nearly-closed Al_2O_3 container is a simple and easy (although not so strict) way to change the CO_2 partial pressure during the sintering (see Table 2).

Figure 3 shows SEM photographs of the porous $CaZrO_3$/MgO/1 vol%-Pt composite sintered at 1100°C:

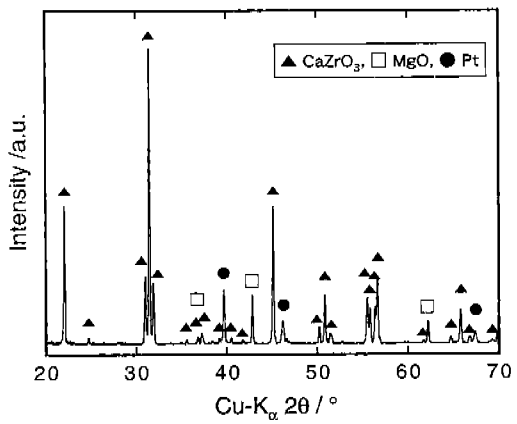

Fig. 2. XRD pattern of the porous $CaZrO_3$/MgO/1 vol%-Pt composite (porosity: 56%) sintered at 1100°C.

Table 2. Effect of the use of Al_2O_3 container on the porosity for the *in situ* composites sintered for 2 h in air.

	Porosity (%)	
	Sintered in nearly open air	Sintered using Al_2O_3 container
$CaZrO_3$/MgO (at 1100°C)	52 [Ref. 9]	56 [Ref.10]
$CaZrO_3$/MgO (at 1300°C)	40 [Ref.9]	47 [Ref.10]
$CaZrO_3$/MgO/Pt (at 1100°C)	28 (this work)	56 (this work)

(a) porosity 28% (without Al_2O_3 container) and (b) porosity 56% (with Al_2O_3 container). For both composites, Pt nano-particles were clearly seen on the $CaZrO_3$ and MgO grains. In addition, a well-developed 3-D network structure was observed for the composite with 56%-porosity. Their pore-size distributions are given in Fig. 4. The $CaZrO_3$/MgO/Pt composite with higher porosity (Fig. 4b) had a narrow distribution with mean size of ~1 μm, similarly to the $CaZrO_3$/MgO composite reported before.[9] On the other hand, that with lower porosity (Fig. 4a) had a slightly wider

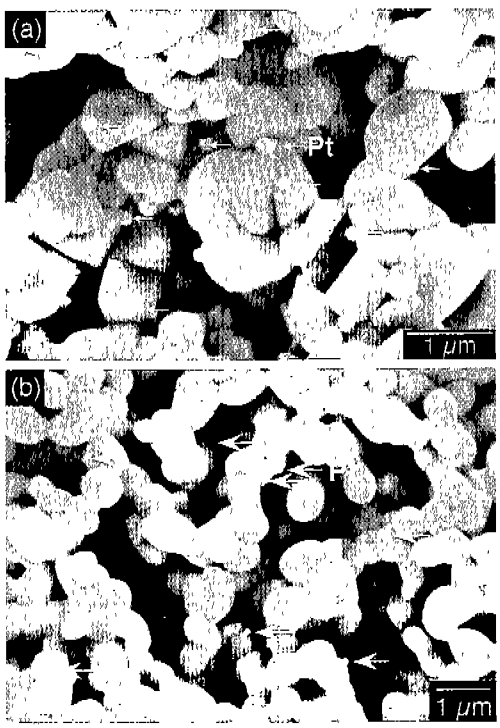

Fig. 3. SEM photographs of the porous $CaZrO_3$/MgO/1 vol%-Pt composite sintered at 1100°C: (a) porosity 28% (without Al_2O_3 container) and (b) porosity 56% (with Al_2O_3 container).

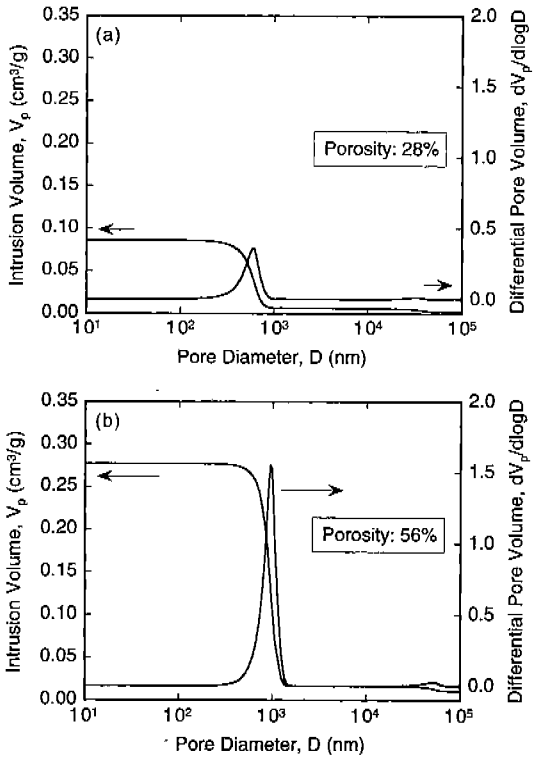

Fig. 4. Pore-size distribution of the porous $CaZrO_3$/MgO/ 1 vol%-Pt composite sintered at 1100°C: (a) porosity 28% and (b) porosity: 56%.

distribution towards smaller size, which can be explained by the progress of localized liquid-phase sintering (see the faceted grains in Fig. 3a).

3.3. Catalytic property of the Pt-dispersed porous composite

Figure 5 shows the NO decomposition behavior of the porous $CaZrO_3$/MgO/Pt (porosity: 56%) composite. In the absence of oxygen, NO direct decomposition (closed circle in Fig. 5) starts at ~500°C. The NO conversion rate increased with increasing temperature and reached 52.3% at 900°C. NO conversion rate dramatically enhanced by the addition of C_2H_4 as a reducing agent (open circle in Fig. 5). The NO reduction starts at ~300°C, and the conversion rate reached 100% at 400°C. However, it dropped drastically with the introduction of excess oxygen (e.g., 2% O_2); the NO conversion rate was 3~4% at maximum both for NO direct decomposition and NO reduction by C_2H_4.

Thus, provided that there is not excess O_2, the porous composite may be applied as a multifunctional filter, i.e., simultaneous hot gas-filtering and de-NO_x in one

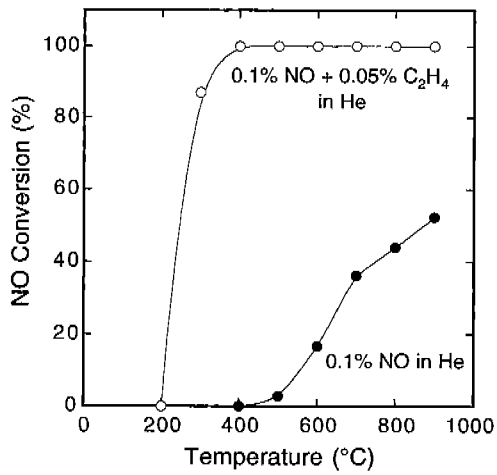

Fig. 5. NO decomposition activity of the porous $CaZrO_3$/ MgO/1 vol%-Pt composite (porosity: 56%) sintered at 1100°C.

component. Although further studies are required to increase the de-NO_x efficiency, it is expected that co-dispersion with another noble metal using a similar *in situ* process (e.g., nano palladium from PdO, or nano rhodium from Rh_2O_3) will be a potential strategy.

4. Summary

A simple platinum nano-dispersion method via *in situ* processing was demonstrated in this paper. Nanosized-platinum-dispersed $CaZrO_3$/MgO porous composites with uniformly open pore structure were synthesized. The composite with higher porosity (56%) had a narrow pore-size distribution with a mean pore size of ~1 μm. Because the composite decreased NO_x concentration, it may be applicable as a filter material with catalytic functions.

Acknowledgement. This work has been Supported by METI, Japan, as part of the Synergy Ceramics Project. The authors are members of the Joint Research Consortium of Synergy Ceramics.

This paper is dedicated to Professor Dr. Koichi Niihara on the occasion of his 60th birthday

References

1. M. Kulmala, V. Riihiluoma and T. Raunemaa: J.

Aerosol Sci., **17** (1986) 973.
2. F. Vyarawalla, P. P. Parikh, H. C. Dak and B.C. Jain: Biomass, **5** (1984) 227.
3. R. R. Judkins, D. P. Stinton, R. G. Smith, E. M. Fischer, J. H. Eaton, B. L. Weaver, J. L. Kahnke and D. J. Pysher: J. Eng. Gas Turbines Power, **118** (1996) 495.
4. Y. M. Jo, R. B. Hutchison and J. A. Raper: Powder Technol., **91**(1997) 55.
5. L. Montanaro: Ceram. International, **25** (1999) 437.
6. H. J. Hwang and M. Awano: J. Eur. Ceram. Soc., **21** (2001) 2103.
7. T. Tanaka, S. Yoshida, R. Kanai, T. Shishido, H. Hattori, Y. Takata and N. Kosugi: J. Phys. IV, Colloq.7 (1997) 913.
8. I. Hattori: Ceramics Japan, **29** (1994) 307.
9. Y. Suzuki, P. E. D. Morgan and T. Ohji: J. Am. Ceram. Soc., **83** (2000) 2091.
10. Y. Suzuki, M. Awano, N. Kondo and T. Ohji: J. Ceram. Soc. Jpn., **109** (2001) 79.
11. Y. Suzuki, H. J. Hwang, N. Kondo and T. Ohji: J. Am. Ceram. Soc., in press.
12. Y. Suzuki, P. E. D. Morgan, T. Sekino and K. Niihara: J. Am. Ceram. Soc, **80** (1997) 2949.
13. Y. Suzuki, P. E. D. Morgan and K. Niihara: Powder Diffraction, **13** (1998) 216.
14. R. Kubo, S. Nagakura, H. Iguchi and H. Ezawa, (Eds.), Encyclopedia of Physics and Chemistry (Rikagaku-Jiten), 4 th Edition, Iwanai, Tokyo, Japan (1987) 501.
15. O. Muller and R. Roy: J. Less-Common Metals., **16** (1968) 129.
16. C. P. Hwang and C. T. Yeh: J. Molecular Catal. A-Chem., **112** (1996) 295.
17. Outokumpu Research Oy (Finland): HSC Chemistry ver 4.0, (1999).